RSC Advances

PAPER

View Article Online
View Journal | View Issue

Cite this: *RSC Adv.*, 2018, **8**, 2586

Novel $CeMo_xO_y$-clay hybrid catalysts with layered structure for selective catalytic reduction of NO_x by NH_3†

Boyang Xu,[abc] Youlin Liu, *[abc] Yuesong Shen*[abc] and Shemin Zhu[abc]

Received 6th November 2017
Accepted 19th December 2017

DOI: 10.1039/c7ra12153a

rsc.li/rsc-advances

A facile method is to prepare novel $CeMo_xO_y$-clay hybrid catalysts with layered structures by using organic cation modified clay as support. During the preparation process, cerium cations and molybdate anions are easily adsorbed and impregnated into the interlamellar space of the organoclay, and after calcination they undergo transformation to highly dispersed $CeMo_xO_y$ nanoparticles within the interlamellar space of the clay. As expected, the prepared $CeMo_{0.15}O_x$-OC-*T* catalysts with layered structures had high selective catalytic reduction (SCR) activity such as high NO_x conversion of >90% in the wide temperature range of 220–420 °C. Meanwhile, they also exhibit high stability and tolerance to water vapor (5 vol%) and SO_2 (200 ppm), demonstrating that these novel catalysts could serve as a good alternative for NH_3-SCR in practical application.

Introduction

Nowadays, great challenges for the effective removal of nitrogen oxides from outgases remains. The selective catalytic reduction of NO_x with NH_3 (NH_3-SCR) has been proven to be an effective approach for NO reduction from stationary sources. However, the commercially available V_2O_5–WO_3 (MO_3)/TiO_2 catalysts has several inevitable drawbacks such as easy sublimation and loss of V_2O_5 in the application process as well as biological toxicity, and narrow operation temperature window.[1] Therefore, it is desirable to develop a highly efficient, stable and environmental-friendly catalyst.

Recently, cerium-based catalysts had becoming promising candidate due to its nontoxic, high surface area and remarkable oxygen storage capacity in SCR reaction as support,[2,3] promoter,[4] or main active component.[5–7] However, pure CeO_2 possesses poor SCR activity,[8] it is necessary to adjust their surface acidity,[9,10] redox property[11,12] and structure stability[13] of CeO_2-based catalysts to improve the SCR performance.

Layered clays such as montmorillonite (MMT), are one type of clay minerals in where negatively changed aluminosilicate layers having an excess of negative charge that interacted strongly by electrostatic forces with charge balancing cations, typically alkali metal ions, located in interlamellar space. In spite that layered clay are constituted by layers with large surface area, the interlamellar space is generally not accessible to any substrate due to the strong electrostatic interaction.[14] It is found that pillaring interlayered clays (PILC) in which inorganic metal polycations were introduced and intercalated in the interlamellar space of the swelling clay and attracted much attention in application of NH_3-SCR.[15] These different pillared clays catalysts such as vanadium supported WO_3–TiO_2-pillared clays,[16] Cu/Co modified Al_2O_3/TiO_2-pillared MMT,[17,18] Fe modified TiO_2-pillared MMT,[19,20] Mn–Ce supported TiO_2-pillared clays,[21] Mn–Ce supported Al_2O_3–CrO_2-pillared clays,[22] exhibited more improved SCR activities because these intercalation (pillaring) could provide a possibility of tailoring porous structure, redox and acidic properties of clay. However, these catalysts either toxic, or had still low catalytic activity, or complicated preparation process, limiting their practical application for NH_3-SCR.

Here, we first presented a facile and cost-effective approach to prepare the novel $CeMo_xO_y$-clay hybrid catalyst with layered structure, designed by using organic cations modified clay (denoted as OC) as support and CeMo mixed oxides as active component. As shown in Scheme 1, organic cations (such as the

[a]College of Materials Science and Engineering, Nanjing Tech University, Nanjing 210009, China. E-mail: youlinliu@njtech.edu.cn; sys-njut@163.com

[b]Jiangsu Collaborative Innovation Center for Advanced Inorganic Function Composites, Nanjing Tech University, Nanjing 210009, China

[c]Jiangsu National Synergetic Innovation Center for Advanced Materials, Nanjing Tech University, Nanjing 210009, China

† Electronic supplementary information (ESI) available. See DOI: 10.1039/c7ra12153a

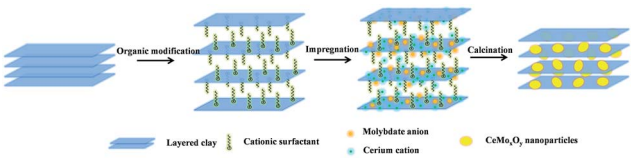

Scheme 1 Illustration for the preparation of $CeMo_xO_y$-OC-*T* catalysts.

quaternary ammonium surfactants) modified the clay such as Na-based MMT (denoted as NaC) with layered structure by ion exchange, where organic cations could increase the basal space of clay. Then molybdate anion could be adsorbed into the layered structure by the organic cations, meanwhile, cerium ion also could uniformly insert the interlamellar space of clay. After calcination, the intercalated ions were converted into the corresponding metal oxides, well dispersed $CeMo_xO_y$ nanoparticles with a particle size of 10–20 nm are hosted in the clay matrix (denoted as $CeMo_xO_y$-OC-*T*, *T*: calcination temperature). The layered structure of novel catalyst has more responsibilities to high SCR activity. In addition, the organic cations also could decrease alkali metal content (Na, K) of clay by ion exchange, further improving SCR activity.

Experimental

Chemicals and materials

All reagents used were of at least analytical grade without further purification. Cerium nitrate, ammonium molybdate, oxalic acid, octadecyltrimethyl ammonium bromide, cetyltrimethyl ammonium bromide, polyoxyethylene were obtained from Aladdin Reagent Co. Na-based MMT with its cation exchange capacity (CEC) of 0.82 mmol g^{-1} was supplied by FengHong Company (Zhejiang, China).

Synthetic procedures

Organoclay (OC) was prepared by using Na-based MMT (NaC) into organic modifiers solution by ion exchange. The organic modifier solution contained octadecyltrimethyl ammonium cations (70 wt%) and cetyltrimethyl ammonium cations (30 wt%). 10 g Na-based MMT was added into 150 mL of organic modifier solution, and turbid solution was stirred for 24 h, and then the solid was filtered, washed and dried at 80 °C for 24 h, and this process of ion exchange was repeated three times, and the cation exchange capacity (CEC) of the obtained organoclay was 1.35 mmol g^{-1}. 1.6 g ammonium molybdate and 25.4 g $Ce(NO_3)_4$ were dissolved into the 150 mL of oxalic acid solution (1.5 wt%). After stirring 30 min, and the above organoclay was added into the above solution and stirred at 20 °C for 24 h to obtain the suspicion. Then the suspicion was dried at 80 °C for 6 h, and then added 0.1 g polyoxyethylene to the suspicion, finally the mixture was molded and dried at 100 °C for 5 h. The different catalysts were obtained at different calcination temperature (such as 450, 500, 550, 600, 650 °C) for 4 h (denoted as $CeMo_xO_y$-OC-*T T*: calcination temperature), respectively. For comparison, the catalyst with NaC as support was also prepared with the above similar conditions (denoted as $CeMo_xO_y$-NaC-*T*).

Catalyst characterization

Scanning electron microscopy (SEM: Nanosem 430) was used to analyse the morphology of samples. Transmission electron microscopy (TEM) was performed on Jeol-2100f. All samples subjected to TEM measurements were ultrasonically dispersed in ethanol at 30 min and dropped on copper grids.

The crystal structure of catalysts were determined by the powder X-ray reflection diffraction (XRD) performed on Rigaku DMAX-RB with a radiation of Cu Kα ($\lambda = 1.5406$ Å). The 2θ scans cover the range 5–80° with a step size of 0.02° and a scan rate of 5° min^{-1}.

Nitrogen adsorption and desorption isotherms were measured on TristarII3020 at 77 K. Specific surface area was calculated by BET method, pore-size distribution was calculated from the adsorption branch using BHJ method, and total pores volume was obtained at P/P_0 of 0.97.

Temperature-programmed reduction by hydrogen (H_2-TPR) were carried out on Micromeritics AutochemII2920 chemisorption analyzer. Prior to each experiment, samples were pretreated in helium stream at 300 °C for 2 h and then cooled to 50 °C. After switching to 10 vol% H_2 in helium balance with the gas rate of 50 mL min^{-1}, TPR experiment started at a ramping rate of 10 °C min^{-1} up to 800 °C.

Temperature-programmed desorption of ammonia (NH_3-TPD) data were collected using Micromeritics AutochemII2920 chemisorption analyzer. Prior to each experiment, samples were pre-treated in helium stream at 300 °C for 2 h and then cooled to 50 °C for ammonia adsorption. NH_3 in helium balance (50 mL min^{-1}) was introduced for 1 h to achieve adsorption equilibrium. Then the samples were purged with helium for 1 h to remove the weakly adsorbed ammonia. Finally ammonia was desorbed using helium at a flow rate of 50 mL min^{-1} from 50 °C to 700 °C with a ramping rate of 10 °C min^{-1}.

Catalyst performance test

The catalytic activities of various catalysts for NH_3-SCR of NO were carried out in a fixed-bed quartz reactor (i.d. = 45 mm) containing 10 mL of catalyst. The feed gas mixture consists of 850 ppm NO, 850 ppm of NH_3, 10 vol% of O_2. A total flow rate of 830 mL min^{-1} was maintained for all experiments with N_2 as balance gas, and the corresponding space velocity was 5000 h^{-1}. The concentration of NO, NO_2 in the inlet and outlet was measured by a flue gas analyzer (HORIBA METRON, S48 32/HMT). All measured data were collected after 1 h when the SCR of NO by NH_3 reached a steady state at each temperature. NO_x conversion (η) was obtained by following equation:

$$\eta = \left(1 - \frac{[NO_x]_{outlet}}{[NO_x]_{inlet}}\right) \times 100\% \quad [NO_x] = [NO] + [NO_2]$$

Poisoning and regeneration of catalysts

The poisoning of water vapor (and/or 200 ppm SO_2) was investigated by introducing 5 vol% H_2O (and/or 200 ppm SO_2) to the inlet gas (850 ppm NO, 850 ppm NH_3, 10% O_2, balance N_2).

Results and discussion

The X-ray diffraction patterns of the $CeMo_xO_y$-OC-550 catalysts with different Mo/Ce molar ratios (0.05, 0.10, 0.15, and 0.20) were first presented in Fig. 1a. For $CeMo_xO_y$-OC-550 catalysts, there are mixed phases including diffraction peaks

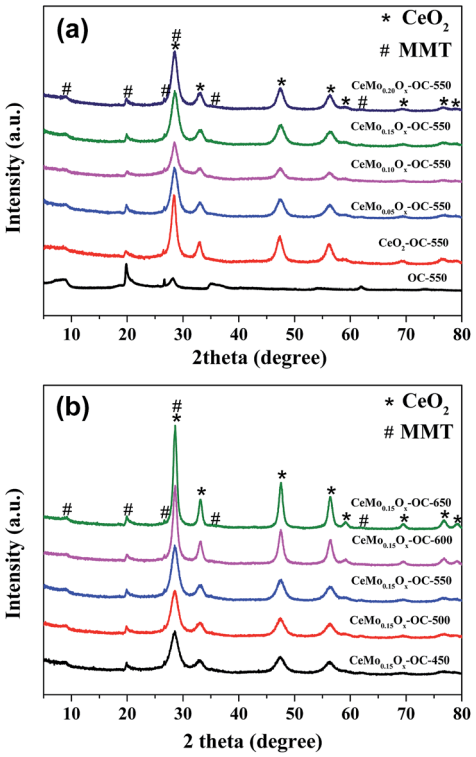

Fig. 1 XRD patterns of (a) $CeMo_xO_y$-OC-550 catalysts with different Mo/Ce ratios, (b) $CeMo_{0.15}O_x$-OC-*T* catalysts with different calcination temperature.

characteristic of cubic CeO_2 structure (JCPDS 65-5923) as well as OC (Fig. 1a). When Mo was added to CeO_2-OC-550, the diffraction peaks intensities of CeO_2 decreased and it is found that no new diffraction peaks appeared, suggesting molybdenum oxide had been well dispersed in CeO_2-OC-550 catalyst. Fig. 1b showed XRD patterns of $CeMo_{0.15}O_x$-OC-*T* catalysts with different calcination temperature (450–650 °C), it can be seen that the diffraction peaks intensities of cerium oxide increased with the increase of calcination temperature. This result implied higher calcination temperature was beneficial to increasing particles size by aggregation and growth.

The morphology of the $CeMo_{0.15}O_x$-OC-550 catalyst was examined by SEM and TEM. Fig. S1† showed that $CeMo_{0.15}O_x$-OC-550 catalyst still maintained the layered structure of clay. Fig. 2 showed that $CeMo_xO_y$ nanoparticles were in the range of 10–20 nm (Fig. 2c and d), and uniformly dispersed within layers of clay (Fig. 2a, b and S2†), which might be responsible for high SCR activity.

The simultaneous TG-DSC analysis (Fig. 3) of the as-prepared $CeMo_{0.15}O_x$-OC precursor showed a continuous weight loss of 43.7% from 40 to 500 °C. The weight loss of 31.5% from 40 to 200 °C accompanied with an exothermic peak at 196 °C could be attributed to desorption of the adsorbed water and intercalated water as well as the part decomposition of the nitrates. The weight loss of 12.2% from 200 to 500 °C companied with an exothermic peak around 245 °C could be attributed to the decomposition of organic species and the combustion of carbon species. After 500 °C, the weight of the precursor has

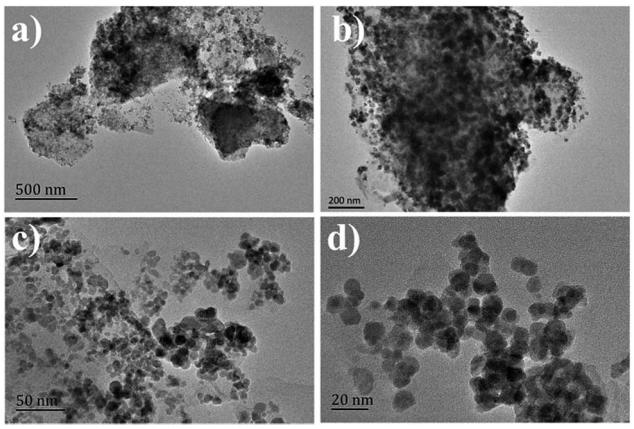

Fig. 2 TEM of the $CeMo_{0.15}O_x$-OC-550 catalyst.

little change, which indicated that the organic species in the sample could be removed after calcined at 500 °C in air.

The catalytic activity of different catalysts was investigated as shown in Fig. 4. For CeO_2-based SCR catalysts, it is found that Mo content had a significant effect on catalytic activity.[23] The influence of Mo/Ce molar ratios on the NO_x conversion of $CeMo_xO_y$-OC-550 catalysts were evaluated at different operating temperature between 175 and 450 °C as shown in Fig. 4, it is shown that Mo/Ce molar ratios had obvious effect on catalytic activity. It is found that the OC-550 as a catalyst exhibited very little catalytic activity for SCR with the maximum NO_x conversion of only 32% at 390 °C, however, when CeO_2 was added into OC-550, the SCR activity of CeO_2-OC-550 catalyst has been greatly improved with its maximum NO_x conversion of 87% at 360 °C. While the addition of a small amount of Mo (Mo/Ce = 0.05) to CeO_2-OC-550, NO_x conversion had significantly increased, indicating Mo played a synergetic role in promoting SCR activity of CeO_2-OC-550 catalyst. The NO_x conversion further increased with the increase of Mo/Ce molar ratios from 0.05 to 0.15, the $CeMo_{0.15}O_x$-OC-550 catalyst exhibited the best SCR activity and widest temperature window with the NO_x conversions of nearby 100% between 240 and 390 °C. When Mo/

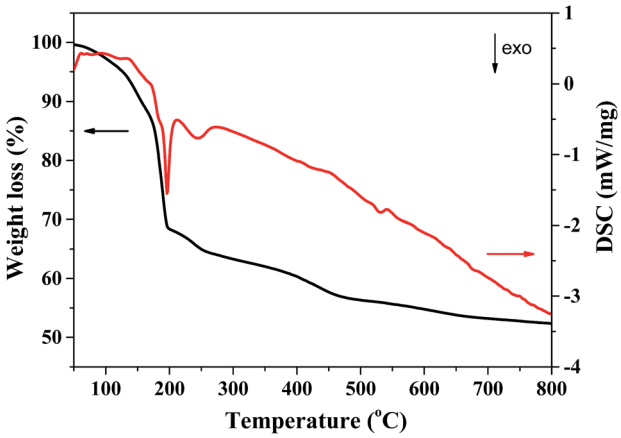

Fig. 3 TG-DSC profiles of the as-prepared $CeMo_{0.15}O_x$-OC precursor.

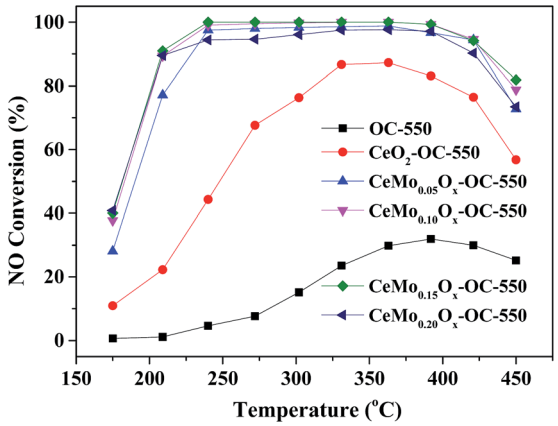

Fig. 4 Catalytic activities of $CeMo_xO_y$-OC-550 catalysts with different Mo/Ce ratios.

Ce molar ratio further increased to 0.20, NO_x conversion began to decrease in operation temperature range.

The surface acidity of catalysts with different Mo/Ce ratios was investigated by NH_3-TPD analysis as shown in Fig. S2a.† It is found that curves of NH_3-TPD for all these catalysts exhibited two desorption peaks at 110 °C and 420 °C, corresponding to weak acid position and strong acid position, respectively. There were negligible changes in the acid strength of these catalysts, indicating that different Mo/Ce ratios had little influence on acid strength. However, the addition of Mo increased the overall amount of acid of catalysts, while amount of acid sites were not changed linearly with the increase of molybdenum content in these catalysts. The surface redox property of catalyst is another important factor for NH_3-SCR. Fig. S2b† presented that all curves of H_2-TPR had one reduction peak for $CeMo_xO_y$-OC-550 catalysts. For the CeO_2-OC-550 catalyst, the reduction peak at about 500 °C could be assigned to the reduction of surface Ce^{4+} (to Ce^{3+}).[24] Comparing with the CeO_2-OC-550 catalyst, the position of reduction peaks had insignificantly changed when the different amount of Mo were added. This result implied Mo was not directly related with the reduction of CeO_2. In addition, the reduction temperature of molybdenum oxides (MoO_3) into MoO_2 was also in the range of 450–560 °C.[25] In addition, the surface chemical states of CeO_2-OC-550 catalyst and $CeMo_{0.15}O_x$-OC-550 catalyst were performed using XPS (Fig. S3†). Fig. S3† showed that the XPS spectra of Ce 3d for both catalysts could be deconvoluted into eight different fitted peaks with two peaks for Ce^{3+} and the remaining six peaks for Ce^{4+}.[26] It is found that when Mo was added into CeO_2-OC-550, the $Ce^{3+}/(Ce^{3+}+Ce^{4+})$ ratio of $CeMo_{0.15}O_x$-OC-550 catalyst increased from 26% to 39%. The increase of the $Ce^{3+}/(Ce^{3+} + Ce^{4+})$ ratio could lead to enhancing SCR activity. This result agreed with previous reports that the value of Ce^{3+} ratio had an important role in improving catalytic activity for NH3-SCR.[27,28]

In practical application, the catalyst for NH_3-SCR should have good thermal stability. Calcination temperature is another important parameter that affects the structure phase of catalyst, and has obvious influence on various characteristic of catalysts such as crystal size, specific surface area and pore structure.[29] Therefore, the $CeMo_{0.15}O_x$-OC-*T* catalyst were calcined at different temperature (450, 500, 550, 600, 650 °C) for 4 h to test thermal stability and the corresponding catalytic results are shown in Fig. 5. All of these catalysts as the increase of calcination temperature from 450 to 650 °C, all these catalyst exhibited high SCR activities, whereas the NO_x conversion had a decline trend at low operating temperature (175–240 °C). It is noted that the NO_x conversion showed little change at high operating temperature (240–450 °C), indicating that the $CeMo_{0.15}O_x$-OC-*T* catalyst exhibited a much superior stable for the high-temperature NH_3-SCR performance. Fig. S4† presented that the different calcination temperature exhibited little influence on both strength and amount of weak acid, reduction property on these catalysts. Researchers had suggested that the weak acid was responsible to high SCR activity.[23] These results illustrated that there were similar weak acid and reduction property with different calcination temperature. Combined the result of XRD patterns, the particle size of catalysts might be responsible to the low-temperature SCR activity.

To understand the influence of organic modification to Na-based MMT (NaC) on SCR activity, we compared $CeMo_{0.15}O_x$-OC-550 catalyst with $CeMo_{0.15}O_x$-NaC-550 catalyst. As shown in Fig. 6a, it is clear that the $CeMo_{0.15}O_x$-NaC-550 catalyst exhibited very low NO_x conversion of only 20–30% in the range of 220–420 °C. However, when NaC were modified by the organic anions, the prepared $CeMo_{0.15}O_x$-OC-550 catalyst exhibited obviously improved SCR activity with NO_x conversion of >90% in the range of 220–420 °C. This result further revealed that the organic modification played a crucial role in the catalytic performance of NH_3-SCR.

Fig. 6b showed that the XRD pattern of the starting clay (NaC) exhibited a peak at 2 theta about 5.6° assigned to the basal spacing $d_{001} = 1.58$ nm, it is worthwhile to note that this value represented the distance between the two layers with the one layer thickness (about 0.96 nm). After being modified by organic cations, the *d*-spacing of the organoclay has obviously increased to 2.14 nm, indicating the organic species were intercalated into the interlayers of clay. This increased *d*-spacing is favorable for the adsorption, impregnation and

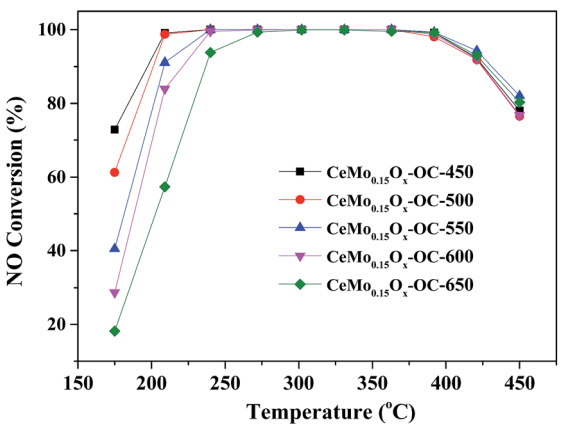

Fig. 5 Catalytic activities of $CeMo_{0.15}O_x$-OC-*T* catalysts with different calcination temperature.

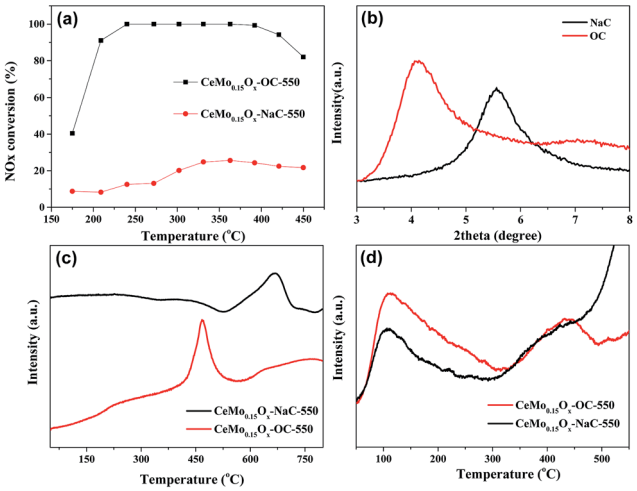

Fig. 6 The NO_x conversion (a), XRD (b), H_2-TPR (c), NH_3-TPD (d) of $CeMo_{0.15}O_x$-OC-550 and $CeMo_{0.15}O_x$-NaC-550 catalysts.

dispersion of active ions in the interlamellar space of clay. Besides, $CeMo_{0.15}O_x$-OC-550 illustrated higher specific surface area and larger pore volume than those of $CeMo_{0.15}O_x$-NaC-550 in Table 1. This high surface area could promote exposure of active phase and utilization efficiency of active sites and large pore volume would favour diffusion of reactants and product, leading to high SCR activity. Table 1 also showed that alkali metal content (Na, K) obviously decreased after organic modification, this result were favorable to the high SCR activity, because high alkali metal could obviously reduce the catalytic activity of NH_3-SCR.[30–32]

Fig. 6c showed that the H_2-TPR profile of $CeMo_{0.15}O_x$-NaC-550 and $CeMo_{0.15}O_x$-OC-550 catalysts. For $CeMo_{0.15}O_x$-NaC-550 catalyst, there is a high reduction peak at 670 °C, which could be assigned to the reduction of the surface Ce^{4+} (to Ce^{3+}). Noticeably, $CeMo_{0.15}O_x$-OC-550 catalyst had the reduction peak at 467 °C, which is much lower than that of $CeMo_{0.15}O_x$-NaC-550 catalyst. This lower reduction peak could be ascribed to the reduction of more well dispersed surface CeO_2 and MoO_3 species, which were favorable for SCR activity. Fig. 6d showed that $CeMo_{0.15}O_x$-NaC-550 catalyst had two desorption processes of ammonia, corresponding to the weak acid and strong acid, respectively. However, in the case of $CeMo_{0.15}O_x$-OC-550 catalyst, the two ammonia desorption processes had little changed, suggesting that organic modification had negligible influence on acid strength for clay, while amount of weak acid had improved obviously, which could be attributed to more well uniformly dispersed $CeMo_xO_y$ nanoparticles. This result also revealed that weak acid playing an important role in SCR activity, which was agree with previously results for the CeO_2-based SCR catalysts.[27,33]

The SCR activity of catalyst with the different GHSV was also be shown in Fig. 7. It is clear that the increase of GHSV from 5000 to 15 000 h^{-1} resulted in the slight decrease of SCR activity at low temperature especially between 175 and 210 °C, while there was little effect on the high-temperature SCR performance. And $CeMo_{0.15}O_x$-OC-550 catalyst showed rather high NO_x conversion exceeding 90% within a broad operation temperature window from 220 to 420 °C. And GHSV further increased to 20 000, the SCR activity slightly decreased.

It is the typical features that there are water vapor and SO_2 in the real operating conditions for flue gas of power plant. Water vapor is one of the main components in flue gases and often leads to catalyst deactivation. Fig. 8 showed that the influence of 5 vol% H_2O vapor on the NO_x conversion for $CeMo_{0.15}O_x$-OC catalyst at 330 °C. It is shown that the NO_x conversion of $CeMo_{0.15}O_x$-OC catalyst was 100% for 24 h. After adding 5 vol% H_2O at 0.5 h, the NO_x conversion started to decrease from 100% to 98.5%, and still remained stable after 18 h running in the presence of 5 vol% H_2O. When water vapor was cut off, the NO_x conversion quickly recovered to 100% and kept stable for another 5 h, probably due to the reversible deactivation by weak comparative adsorption on the active sites where H_2O vapor competed with NH_3 or NO.[27] These results suggested that this prepared catalyst had high tolerance to water vapor.

As there is still certain amount of residual SO_2 in flue gases, the poisoning effect of SO_2 on this catalyst was investigated (Fig. 8). When 200 ppm of SO_2 was added to the flue gases at 0.5 h, the NO_x conversion of $CeMo_{0.15}O_x$-OC-550 catalyst started to decrease from 100% to 91.7%, and then still kept stable for 91.7% within another 18 h, demonstrating that $CeMo_{0.15}O_x$-OC-550 catalyst had high resistance to SO_2. It is probably that the $CeMo_{0.15}O_x$ nanoparticle has high dispersed interlayers of clay structure, which could enhance the stability of SO_2 poisoning. When SO_2 was cut off at 18.5 h, the NO_x conversion for

Table 1 The physicochemical properties of the different samples

Sample	BET surface area (m^2 g^{-1})	Pore volume (cm^3 g^{-1})	Na content (wt%)	K content (wt%)
OC	61	0.11	0.10	0.39
$CeMo_{0.15}O_x$-OC-550	83	0.16	0.03	0.18
$CeMo_{0.15}O_x$-NaC-550	38	0.07	1.18	0.55

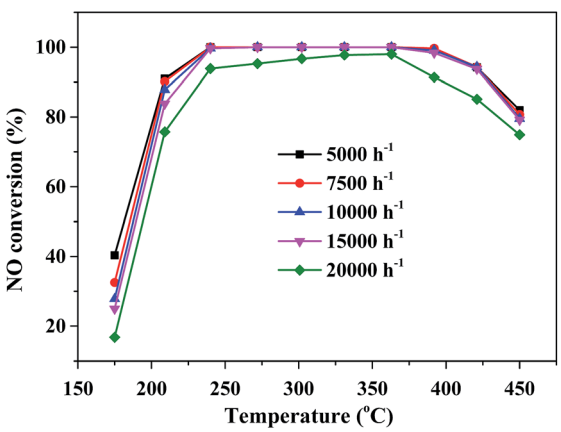

Fig. 7 NO_x conversion of $CeMo_{0.15}O_x$-OC-550 catalyst in the difference space velocity.

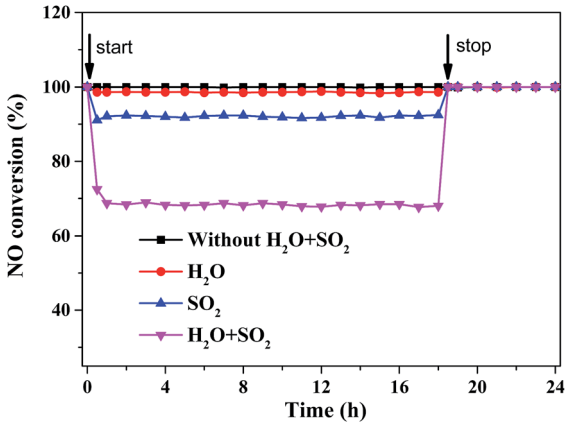

Fig. 8 NO_x conversion of $CeMo_{0.15}O_x$-OC-550 catalyst with different conditions in the presence of 5 vol% H_2O, 200 ppm SO_2 and 5 vol% H_2O + 200 ppm SO_2, respectively, at 5000 h^{-1}, 330 °C.

$CeMo_{0.15}O_x$-OC-550 has quickly recovered to 100%. This result suggested that SO_2 also led to reversible deactivation on the active sites of $CeMo_{0.15}O_x$-OC-550 catalyst by weak comparative adsorption with NH_3 or NO. This data again demonstrated our catalyst possessed high resistance to SO_2. In addition, after adding 5 vol% H_2O and 200 ppm SO_2 to the system simultaneously, the NO_x conversion further decreased about 68%, suggesting the synergistic deactivating effect of H_2O and SO_2 had inhibited the catalytic performance of $CeMo_{0.15}O_x$-OC-550. It is believed that water vapor and SO_2 could inhibit the adsorption and activation of NH_3 & NO on the active sites, leading to an obvious decline of the NO_x conversion.[23] Noticeably, the NO_x conversion had almost been unchanged in the next 18 h. Once water vapor and SO_2 were removed, the NO_x conversion for $CeMo_{0.15}O_x$-OC-550 also recovered quickly to 100% and stable for another 5 h, these result indicated that water vapor and SO_2 had insignificant effect for catalytic active structure of this catalyst, demonstrating that our catalyst possessed good resistance to the co-existence of water vapor and SO_2.

Conclusions

In summary, a facile method was presented to prepare $CeMo_xO_y$-based clay hybrid catalyst with layered structure. With organic cations modified clay as support, after a simple adsorption and impregnation of cerium cations and molybdate anions, and calcination at high temperature, well-dispersed $CeMo_xO_y$ nanoparticles in the layered matrix of clay were prepared and exhibited high and stable SCR performance, presenting the promising potential as candidate for NH_3-SCR. This excellent SCR activity could be attributed to novel layered structure, well-dispersed $CeMo_xO_y$ nanoparticles and lower alkali metal content.

Conflicts of interest

There are no conflicts to declare.

Acknowledgements

This work is financially supported by the Natural Science Foundation of Jiangsu Province of China (No. BK20160982).

References

1 C. Tang, H. Zhang and L. Dong, *Catal. Sci. Technol.*, 2016, **6**, 1248.
2 K. Cheng, J. Liu, T. Zhang, J. Li, Z. Zhao, Y. Wei, G. Jiang and A. Duan, *J. Environ. Sci.*, 2014, **26**, 2106.
3 M. Sakai, Y. Nagai, Y. Aoki and N. Takahashi, *Appl. Catal., A*, 2016, **510**, 57.
4 X. Wang, S. N. Zhao, Y. B. Zhang, Z. Wang, J. Feng, S. Y. Song and H. J. Zhang, *Chem. Sci.*, 2016, **7**, 1109.
5 Y. Geng, W. Shan, S. Xiong, Y. Liao, S. Yang and F. Liu, *Catal. Sci. Technol.*, 2016, **6**, 3149.
6 Y. Shen, S. Zhu, T. Qiu and S. Shen, *Catal. Commun.*, 2009, **11**, 20.
7 L. Chen, J. Li, M. Ge and R. Zhu, *Catal. Today*, 2010, **153**, 77.
8 S. Yang, Y. Guo, H. Chang, L. Ma, Y. Peng, Z. Qu, N. Yan, C. Wang and J. Li, *Appl. Catal., B*, 2013, **136–137**, 19.
9 Y. Shen, *RSC Adv.*, 2012, **2**, 5957.
10 B. Han, Y. Shen, S. Zhu, Y. Liu and S. Shen, *J. Rare Earths*, 2016, **34**, 1010.
11 M. Salazar, S. Hoffmann, L. Tillmann, V. Singer, R. Becker and W. Grünert, *Appl. Catal., B*, 2017, **218**, 793.
12 H. Wang, Z. Qu, H. Xie, N. Maeda, L. Miao and Z. Wang, *J. Catal.*, 2016, **338**, 56.
13 S. Gillot, G. Tricot, H. Vezin, J.-P. Dacquin, C. Dujardin and P. Granger, *Appl. Catal., B*, 2017, **218**, 338.
14 S. Navalon, M. Alvaro and H. Garcia, *Appl. Catal., B*, 2010, **99**, 1.
15 T. Grzybek, *Catal. Today*, 2007, **119**, 125.
16 W. Ferjani, L. K. Boudali, G. Delahay and C. Petitto, *Chem. Lett.*, 2016, **45**, 872.
17 L. Chmielarz, P. Kuśtrowski, M. Zbroja, B. Gil-Knap, J. Datka and R. Dziembaj, *Appl. Catal., B*, 2004, **53**, 47.
18 J. L. Valverde, A. de Lucas, F. Dorado, A. Romero and P. B. García, *J. Mol. Catal. A: Chem.*, 2005, **230**, 23.
19 L. S. Cheng, R. T. Yang and N. Chen, *J. Catal.*, 1996, **164**, 70.
20 R. Q. Long and R. T. Yang, *J. Catal.*, 1999, **186**, 254.
21 Y. Wang, B. Shen, C. He, S. Yue and F. Wang, *Environ. Sci. Technol.*, 2015, **49**, 9355.
22 D. Chen, C. Cen, J. Feng, C. Yao, W. Li, S. Tian and Y. Xiong, *J. Chem. Technol. Biotechnol.*, 2016, **91**, 2842.
23 S. Ding, F. Liu, X. Shi, K. Liu, Z. Lian, L. Xie and H. He, *ACS Appl. Mater. Interfaces*, 2015, **7**, 9497.
24 S. Zhan, H. Zhang, Y. Zhang, Q. Shi, Y. Li and X. Li, *Appl. Catal., B*, 2017, **203**, 199.
25 V. O. O. Gonçalves, C. Ciotonea, S. Arrii-Clacens, N. Guignard, C. Roudaut, J. Rousseau, J.-M. Clacens, S. Royer and F. Richard, *Appl. Catal., B*, 2017, **214**, 57.
26 C. Zhu, T. Ding, W. Gao, K. Ma, Y. Tian and X. Li, *Int. J. Hydrogen Energy*, 2017, **42**, 17457.
27 W. Yan, Y. Shen, S. Zhu, Q. Jin, Y. Liu and X. Li, *Catal. Lett.*, 2016, **146**, 1221.

28 D. W. Kwon, K. B. Nam and S. C. Hong, *Appl. Catal., A*, 2015, **497**, 160.
29 B. Guan, H. Lin, L. Zhu, B. Tian and Z. Huang, *Chem. Eng. J.*, 2012, **181**, 307.
30 Y. Shen and S. Zhu, *Catal. Sci. Technol.*, 2012, **2**, 1806.
31 S. Boxiong, Y. Yan, C. Jianhong and Z. Xiaopeng, *Microporous Mesoporous Mater.*, 2013, **180**, 262.
32 Y. Peng, J. Li, X. Huang, X. Li, W. Su, X. Sun, D. Wang and J. Hao, *Environ. Sci. Technol.*, 2014, **48**, 4515.
33 Y. Shen, Y. Su and Y. Ma, *RSC Adv.*, 2015, **5**, 7597.